Study the effects of the microstructure and microhardness on the external joint welding of stainless steel 316 pipe in sea water

Mohamed. R. Budar Mohamed. Etuohami. Swei Sami. Abdullah. Almashat

Fathi. Rabie. Ashou

College of Engineering Technology-Janzour

Drmohmmed51@gmail.com Mohamedtuhami106@gmail.com _Ashourfathi929@gmail.com

Abstract:
Austenitic stainless steels are very popular due to their high strength properties, ductility, excellent corrosion resistance and work hardening. This paper presents the test results for joining AISI 316 austenitic steel. The technologies used for joining were the most popular welding techniques such as TIG (welding with a non-consumable electrode in the shield of inert gases),
The objectives of this research is to study the effect of welding parameters on the microstructural features and the micro hardness austenitic stainless steel 316 pipes.

The welding process of Tungsten inert gas welding (TIG) process with stainless steel filler metalon austenitic stainless steel 316 pipes with outside diameter of 60mm and inside diameter of 55mm and 400mm length was carried using three different welding current of 130A,150A and 180A welding volte of 20V, welding speed and heat input. The welded pipe was left in offshore topside environment for six months. Microstructural examinations in the face, center and root areas of the weld revealed different contents of delta ferrite with skeletal or lathy ferrite morphology. Additionally, the presence of columnar grains at the fusion line and equiaxed grains in the center of the welds was found.
The hardness value of the welded seam in these joints ranges from 101 to 123 HB.

Keywords: AISI 316, Gas Tungsten Arc Welding, microstructure.

الملخص
يحظى الصلب المقاوم للصدأ الأوستنيتي بشعبية كبيرة نظرًا لخصائص القوة العالية والليونة والمقاومة الممتازة للتآكل وتصلب العمل. تعرض هذه الورقة نتائج الاختبار للانضمام إلى الصلب الأوستنيتي .316 AISIوكانت التقنيات المستخدمة في الربط هي تقنيات اللحام الأكثر شيوعا مثل) TIGاللحام بقطب كهربائي غير قابل للاستهلاك في وجود الغازات الخاملة)،
أهداف هذا البحث هي دراسة تأثير متغيرات اللحام على الخصائص البنيوية الدقيقة والصلابة الدقيقة لأنابيب الفولاذ المقاوم

للصدأ الأوستنيتي 316 .

تمت عملية اللحام بعملية اللحام بغاز التنغستن الخامل ((TIGمع حشو الصلب المقاوم للصدأ على أنابيب الصلب المقاوم للصدأ الأوستنيتي 316 بقطر خارجي 60 ملم وقطر داخلي 55 ملم وطول 400 ملم باستخدام ثلاثة تيارات لحام مختلفة 130 أمبير و150 أمبير و180 أمبير. 20 فولت، سرعة اللحام وإدخال الحرارة. تم ترك الأنبوب الملحوم في بيئة سطح البحر لمدة ستة أشهر.
كشفت فحوصات البنية المجهرية في مناطق الوجه والوسط والجذر للحام عن محتويات مختلفة من فريت الدلتا مع مورفولوجيا الفريت الهيكلي أو الرغوي. بالإضافة إلى ذلك، تم العثور على وجود حبيبات عمودية عند خط الالتحام وحبيبات متساوية المحاور في مركز اللحامات.
تتراوح قيمة صلابة التماس الملحومة في هذه الوصلات من 101 إلى 123 .HB

1.Introduction

Stainless steels are widely used in many manufacturing industries. The Stainless steels are mainly categorized into austenitic, ferritic, martensitic and duplex. Austenitic steels are the steels which have the primary phase as austenite they are generally face centered cubic crystal (FCC). Hardening of Austenitic steel using normal heat treatment is difficult. Ferritic steels are the steels which have the primary phase as ferrite they are generally body centered cubic crystal (BCC), they are generally less ductile when compared to austenitic steel and it also cannot be hardened by heat treatment. The microstructure of martensite was first discovered by German, metallurgist named Adolf Martens around the year 1890, Quenching and cooling below 450 degrees can transform martensite into austenite steel. The major composition of SS is chromium and nickel due to the presence of chromium it makes SS a corrosion resistant metal. The main concept of this project is to introduce the heat to the metal surface and due to raise in the heat input the properties of the metal will change automatically. This heat input can be given to the metal by different types of modes. The heat input can be changed by altering the current with respect to voltage. The voltage and current are noted down and the heat input can be found by calculating in formula. After applying heat on the metal surface the specimen in prepared according to the ASTM standard norms for the microstructural studies were carried out, the changes on the microstructure of the metal are revealed and the results are analyzed and inferred. In the present world every manufacturing industry has a metallurgical division in order to make feasible study on the metals and materials which are used in the production division in an as the little deviation in microstructure and may have a huge impact in the final outlet product. This research helps to analyze the metals which are used various climatic conditions and their variation in the microstructure of the metal used This project also helps to reveal the variation in the microstructure of the metal due to its climatic conditions. The microstructural studies revealing the dendrites formation and grain formation in the metal which helps to analyze about the metal and information about suitable application of the metal and helps in gaining the better results for those applications. [1-4].

2.literature Review:

Shankar *et al.* [5] demonstrated that the addition of nitrogen in the shielding gas during welding of 316L stainless steel increased hot cracking susceptibility of the weld metal. Weld metal exposed to nitrogen in the shielding gas during welding showed a tendency for coarsening and side branching of the solidification structure, which increased with higher amounts of nitrogen in the shielding gas.

Kwok *et al.* [6] reported that when using a shielding gas containing N2 to stabilize austenite, the probability was higher of forming intermetallic precipitates and nitrides in the weld metal, which would decrease the corrosion resistance.

Enerhaug et al [7] The investigations indicating that chromium may oxidize to Cr2O3 while iron may form less stable oxides such as FeOand Fe3O4 during welding of stainless steel when oxygen is present in the atmosphere. Although inert shielding gas is used, oxygen infiltration may still occur in various amounts. The oxygen infiltration will be sufficient to promote the formation of such high temperature oxides.

3. Experimental Procedure

3.1 Welding machine:

Figure 1 illustrates the TIG welding machine.

Fig. 1: TIG Welding Machine

3.2 Gas Cylinder

Gas cylinder- for TIG welding argon gas is supplied to the welding torch with a particular flow rate so that an inert atmosphere formed and stable arc created for welding. Gas flow is control by regulator and valve. The argon gas cylinder is shown in figure 2.

Fig. 2: Argon gas cylinder

3.3 Welding Torch

TIG and Torches Feature Silicone Rubber torch bodies to reduce accidental damage during use the loss of high frequency signal due to torch body cracking related to hard body plastic torch. The TIG Welding Torch is shown in figure 3.

Fig. 3: TIG Welding Torch

3.4 Electrode & Filler Rod

The electrode used in TIG is made of tungsten or a tungsten alloy, because tungsten has the highest melting temperature among pure metals, at 3,422 °C.

As a result, the electrode is not consumed during welding, though some erosion (called burn-off) can occur. Electrodes can have either a clean finish or a ground finish—clean finish electrodes have been chemically cleaned, while ground finish electrodes have been ground to a uniform size and have a polished surface, making them optimal for heat conduction. The diameter of the electrode can vary between 0.5 and 6.4 millimeters and their length can range from 75 to 610 millimeters/

For this research the electrode E308 has been used, the chemical composition of the electrode is illustrating below:

2.4 Welding parameters

A. Welding Current, It controls the melting rate of the electrode and thereby the weld deposition rate. It also controls the depth of penetration and thereby the extent of dilution of the weld metal by the base metal.

B. Welding Speed and Heat input Welding speed is the linear rate at which the arc moves with respect to plate along the weld joint. Welding speed generally conforms to a given combination of welding current and voltage. If welding speed is more than required heat input to the joint decreases, less filler metal is deposited than required, Reinforcement height decreases'. If welding speed is slow, heat input rate increases, Weld width increases and reinforcement height also increases more convexity [8].

C. Gas flow rate argon is the most used TIG shielding gas. Argon is used in welding of carbon and stainless steels and low thickness aluminum alloys components. Gas flow rate influence the welding speed and improves process tolerance. Heat input rate=60VI/v J/mm V=arc voltage in volts I=welding current in ampere, v =speed of welding in mm/min

2. Materials and Experimental Procedures

2.1. Materials

The material used in this investigation was stainless steel 316(AISI 316) and nine pipes of outer diameter of 60m, inner diameter of 55mm and lenght400mm was used as work–piece materials. The chemical compositions of the material used are shown in Table1.

Table 1 Chemical Composition of AISI 316 (wt.%)

Grade	C (%)	Cr (%)	Mn (%)	Mo (%)	N (%)	Ni (%)	P (%)	Si(%)	S (%)
316	≤ 0.08	16.0–18.0	≤ 2.0	2.0–3.0	≤ 0.10	10.0–14.0	≤ 0.045	≤0.75	≤0.03

. The filler wires used to transfer the extra material to fill the gap between the joints of same composition of base metal.

In this experimental work, the filler wire of SSE308L grade is selected for welding the stainless steel 316 specimens because of its good, similar physical, mechanical properties and chemical compositions for obtaining the best weld joint. The chemical composition of SSE308L filler wire is shown in table 2.

Table 2: Chemical Composition of SSE308L Filler Wire

Chemical composition %wt							
Material	**C**	**Si**	**Mn**	**Cr**	**S**	**P**	**Ni**
SSE308L	0.01	0.40	1.6	20	0.20	0.4	10

experimental work TIG welding is used to weld stainless steel 316 with use of 4043 graded filler wire. The stainless steel 316(AISI 316) and nine pipes of outer diameter of 60m, inner diameter of 550mm and lenght400mm was used as work–piece materials. The work piece is shown in figure 4.

Fig. 4: Illustrate the TIG pipe welding specimen.

3.6 The welding parameters:

Filler wire – SSE308L graded

Welding current – 220 amp
Arc voltage – 20 volts
Travelled distance of weld bead – 50 mm
In this study, welding speed is calculated for each welded specimen by measuring the varied arc time. Generally, welding speed is determined by mathematical formula:
Welding speed (mm/min) = Travelled/Arc Time
Heat input or Energy is calculated from mathematical formula:
Heat input(joule/mm) =60 VI/S.
Where,
V = Arc voltage in volt
I = Welding current in ampere
S = Welding speed in mm/min.

Readings of depth of penetration obtained by measuring instrument after cutting each specimen perpendicular to weld bead direction and the values of depth of penetration with respect to input parameters such as welding speed, gas flow.

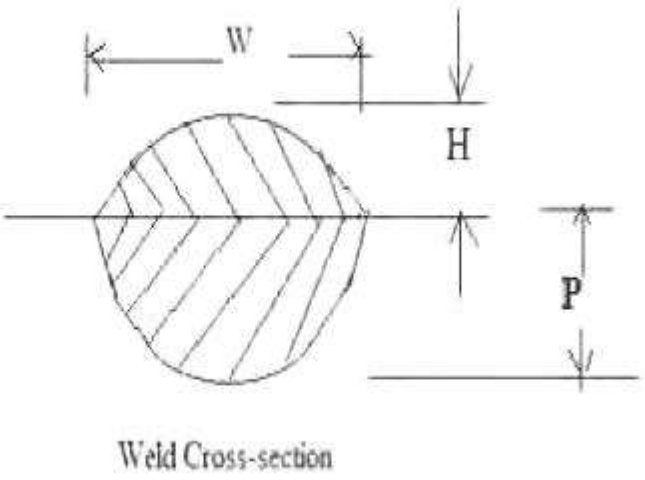

Fig. 5. Weld bead geometry

W- Weld Width, P- Penetration, H- Reinforcement
During the welding process, Current = 210, Amp Terminal voltage = 20 V
Only Gas flow rate was varied during the welding. Welding speed was calculated for each welded specimen. Having finished the welding processes, in order to measure the depth of penetration, welds were cut perpendicular to the direction of welding on power hacksaw. Then with the help of measuring instrument, depth of penetration of welded specimens was measured.

5.Microstructural

Seawater chloride ion, and the chloride ion is the major factor, of which stainless steel pipe occurs corrosion in seawater includes lots of. The powerful binding force between chloride ion and metallic bond is very strong, and then chloride ion intrudes easily into passivating film and breaks

passivating film. In the field of stainless steel pipe welded joint and nearby, as affected by heat cycle effect of welding, the welded joint field's metallurgical structure varies very much. Therefore, besides for destruction of chloride ion, the field tends to occurring local selective corrosion and inter crystalline corrosion. Therefore, minute sulfide is scattered around the MnS compound, and it promotes corrosion easily. So to sum up, lack of Mn element in WZ, the ability of resistant corrosion in WZ doesn't vary; the ability of resistant corrosion in HAZ is worse than others. Without the process of recrystallization, the ability of resistant corrosion also doesn't vary. Elements of Cr, Ni and Mo are the essential elements of seawater corrosion resistant steel, and the variation of their elements' content affects directly the abilities of its steel's resistant corrosion Especially, the effect of corrosion is more serious after welding without heat treatment.

Figure 6,7 and 8 shows that the microstructure of a TIG joint. In the case of the root bead and the center bead, the amount of energy introduced was similar, while the linear energy was lower by 0.39 kJ/min in the face bead. The difference in the amount of energy causes different grain sizes to be visible in individual layers of the weld, which decrease towards the face of weld. The observations showed a heat-affected zone, the average width of which was 174 μm, while the joint area covered an area of 42 mm^2. The width of the heat-affected zone obtained in the welded joint using the TIG method is approximately 60 μm larger than the HAZ zone obtained using the MIG method. This is caused by the introduction of a larger amount of energy and is related to the different cooling speed. Microstructure researches using light microscopy showed the absence of cracks, bubbles, sticking, inclusions, proper penetration and correct formation of the face and root of the weld. Different amounts of heat introduced and different crystallization rates of the joint when applying subsequent layers are visible as narrow zones of enriched delta ferrite. In the areas of the fusion line welding, delta ferrite can be observed, with an elongated morphology, while towards the weld axis the morphology of lamellar ferrite transforms into skeletal ferrite. The difference in morphology and distribution of delta ferrite occurs in the weld axis. In the root and center of the weld, the delta ferrite is "finer" and is evenly distributed compared to the delta ferrite present in the face of the weld. This is due to the uneven cooling speed of individual beads. In these areas, as in the different morphologies of delta ferrite can be distinguished: lathy and skeletal. Skeletal ferrite occurs both in the areas of the fusion line and in the face of weld, where the solidification rate is higher compared to other areas of the weld. In the root of the weld, the skeletal ferrite crystals are arranged in parallel, while in the areas of the center and face of the weld there is no clear orientation. The element distribution map made in the central part of the weld confirms the presence of delta ferrite rich in chromium and molybdenum and the occurrence of titanium carbides.

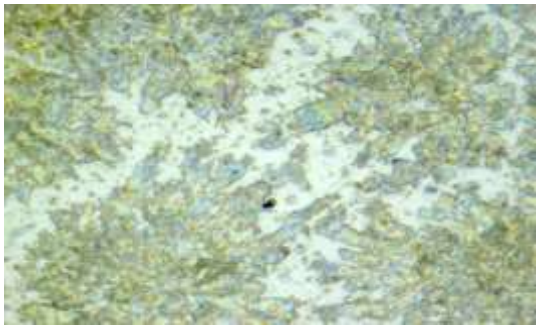

Fig. 6: Micrographs at the cross section of the welding carried out with different Welding speed for welding current of 130 A

Fig. 7: Micrographs at the cross section of the welding done with different

Welding speed for welding current of 150 A

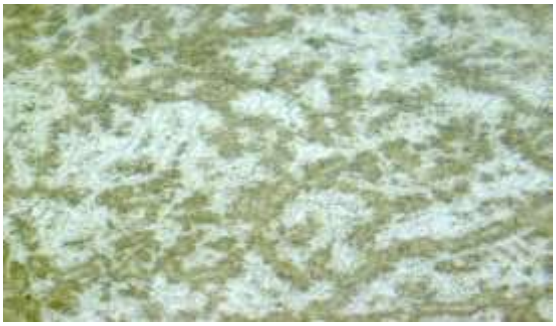

Fig. 8: Micrographs at the cross section of the welding done with different

Welding speed for welding current of 170 A

6. The effect of hardness on the TIG welding of stainless steel 316

The hardness distribution profile on the transverse cross -section of the joint, welded 9 specimens. The hardness values of base metals 108 HB. The micro hardness of welding area was higher than that of base metal due to fast cooling rate. The occurrence could be probably attributed to the dendritic grain of the TIG welding process of stainless steel 316. An inhomogeneous distribution of hardness values was observed in the weld area (WA). The higher the hardness value in the WA relative to base metal was primarily associated with the formation of solid to liquid

transformation dendritic grains observation. The higher values of the hardness at the weld zone were reached to123 HB and lower hardness value was 101 HB.

Main effect plots for micro hardness are as shown in figure 9. In order to see the effect of process parameter on micro hardness using nine samples nine samples and experiments are performed and the experimental data are given in table 3. It is clear that as groove angle increasing the hardness also increasing. It was observed that as root face goes up to 1.5 mm the micro hardness will be decreasing. If the roots face goes up to 2 mm the micro hardness will be increasing. It was observed that as root gap increasing the hardness also will increase.

Table: 3 Hardness of TIG welding for stainless steel 316

Experiment number	**1**	**2**	**3**	**4**	**5**	**6**	**7**	**8**	**9**
Hardness (HB)	**101**	**123**	**108**	**116**	**103**	**104**	**110**	**106**	**104**

Fig.9 shows that the maximum value of hardness was obtained at experiment number two with welding current of 220A and welding volte of 20V.

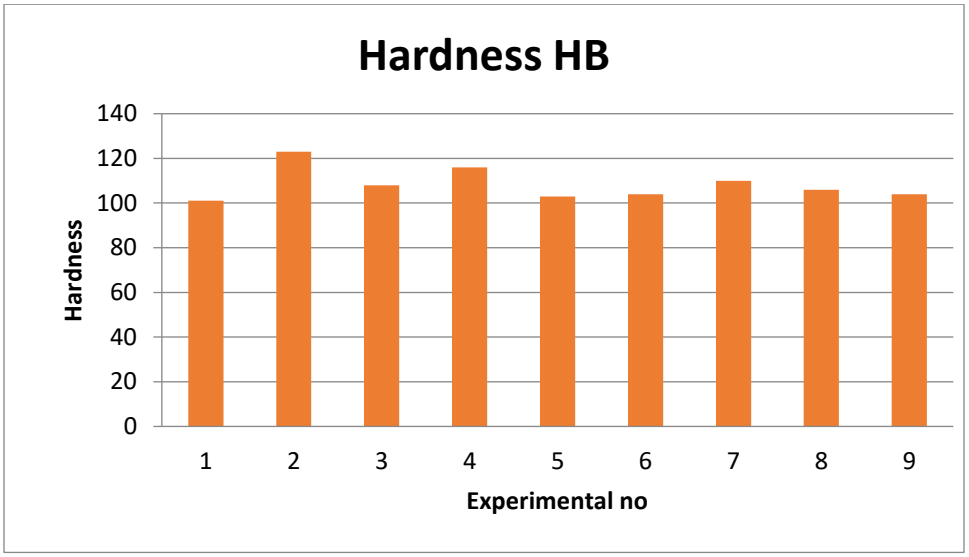

Fig.9. Shows the number of experiments vs hardness

7.Conclusion

TIG Welding of stainless steel 316(AISI 316) pipes of outer diameter of 60m, inner diameter of 55mm has been successfully implemented. The microstructures, hardness profiles have been

discussed specifically. From this study, the Different welding input parameters have changed the microstructure of welded joint.

The following conclusions were drawn from the results of this research:

1. The content of α phase in HAZ is too high and leads to intergranular corrosion, seriously reduces the life of the water pipeline.
2. The content of chromium is low in HAZ and separates out α phase, the corrosion rate is big, and it indicates that the poor chromium causes the localized corrosion acceleration.
3. The stability of inclusion content, Microstructure shape, polarization curve in the weak polarization area indicate the resisted seawater corrosion and nearby have discrepancies, and the ability of HAZ is the worst; when welding it should pay attention to avoiding the appearance of α phase.
4.The hardness value of the welded seam in these joints ranges from 101 to 123 HB.

References

[1] Subodh Kumar, A.S. Shahi [2011] " Effect of heat input on the microstructure and the mechanical properties of gas tungsten arc welded AISI 304 stainless steel joints" [Materials and Design Vol. 32 (2011) pp. 3617–3623].

[2] O.P.Khanna"Welding Technology" Metalloagraphic and Microstructure studies from the "Metallographic and Microstructures"[2004] by ASM HAND BOOK.

[3] "Dr. Sc. Almaida Gigović-Gekić1, Dr.Sc. Mirsada Oruč2, Dr. Sc. Mirko Gojić3 [2011] "Determination Of The Content Of Delta Ferrite In Austenitic Stainless Steel Nitronic 60" [Materials and technology, Vol. 46 (2012) No. 5, pp. 519–523]. Dekker, C. (1999). Carbon Nanotubes as Molecular Quantum Wires. Physics Today, 52(5), 22.

[4] A. F. PADILHA and P. R. RIOS [2002] "Decomposition of Austenite in Austenitic Stainless Steels" [ISIJ International, Vol. 42 (2002), No. 4, pp. 325–337].

[5] Shankar, V., *et al*., *Effect of nitrogen addition on microstructure and fusion zone cracking in type 316L stainless steel weld metals,* Materials Science and Engineering: A, 343 (1), 2003, p. 170-

[6] Kwok, C., *et al*., *Pitting and galvanic corrosion behavior of laser-weldedstainless steels,* Journal of p. 168-178.materials processing technology, 176 (1-3), 2006,

[7] Enerhaug, J., *A study of localized corrosion in super martensitic stainless steel weldments*, Doctoral Thesis, The Norwegian University of Science andTechnology (NTNU), Department of Machine Design and Materials Technology, 2002.

. [8] Degerbeck, J. and E. Wold, *Some aspects pit of the influence of manganese in austenitic stainless steels,* Materials and Corrosion, 25 (3), 1974, p. 172-174